Heterogeneous structure around the rupture area of the 2003 Tokachi-oki earthquake (Mw=8.0), Japan, as revealed by aftershock observations using Ocean Bottom Seismometers

Yuya Machida[a*], Masanao Shinohara[b], Tetsuo Takanami[a], Yoshio Murai[a], Tomoaki Yamada[b], Naoshi Hirata[b], Kiyoshi Suyehiro[c], Toshihiko Kanazawa[b], Yoshiyuki Kaneda[c], Hitoshi Mikada[d], Shin'ichi Sakai[b], Tomoki Watanabe[c], Kenji Uehira[e], Narumi Takahashi[c], Minoru Nishino[f], Kimihiro Mochizuki[b], Takeshi Sato[c], Ei'ichiro Araki[c], Ryota Hino[f], Kouichi Uhira[g], Hajime Shiobara[b], Hiroshi Shimizu[e]

[a] *Institute of Seismology and Volcanology, Hokkaido University, N10 W8 Kita-ku, Sapporo 060-0810, Japan*

[b] *Earthquake Research Institute, University of Tokyo, Tokyo, 113-0032, Japan*

[c] *Japan Agency for Marine-Earth Science and Technology, Yokosuka, 237-0061, Japan*

[d] *Department of Civil and Earth Resources Engineering, Kyoto University, Kyoto, Japan*

[e] *Institute of Seismology and Volcanology, Kyushu University, Shimabara 855-0843, Japan*

[f] *Graduate School of Science, Tohoku University, Sendai 980-8578, Japan*

[g] *Japan Meteorological Agency, Tokyo 100-8122, Japan*

Revised for Tectonophysics

* Corresponding author

Tel.: +81 11 746 2643, Fax: +81 11 746 7404.

Email address; yuya@mail.sci.hokudai.ac.jp (Y. Machida)

Abstract

Large earthquakes have repeatedly occurred in the area off southeastern Hokkaido Island, Japan, as the Pacific Plate subducts beneath the island, which is on the North American Plate. The most recent large earthquake in this area, the 2003 Tokachi-oki earthquake (Mw = 8.0), occurred on September 26, 2003. In order to investigate aftershock activity in the rupture area, 47 Ocean Bottom Seismometers (OBSs) were quickly deployed after the main shock. In the present study, we simultaneously estimate the hypocenters and 3-D seismic velocity models from the P- and S-wave arrivals of the aftershocks recorded by OBSs. The subducting plate is clearly imaged as a northwest dipping zone in which Vp is greater than 7 km/s, and the relocated hypocenters also show the subducting Pacific Plate. The aftershock distribution reveals that the dip angle of the plate boundary increases abruptly around 90 km from the Kuril Trench. The bending of the subducting plate corresponds to the southeastern edge of the rupture area. The island arc crust on the overriding plate has P-wave velocities of 6-7 km/s and a Vp/Vs of 1.73. A region of Vp/Vs greater than 1.88 was found north of the epicenter of the main shock. The depth of the high Vp/Vs region extends about 10 km upward from the plate interface. The plate boundary just below the high Vp/Vs region has the largest slip at the main rupture. A high Vp anomaly (~ 7.5 km/s) is found in the island arc crust in northeast part of the study area, which we interpret as a structural boundary related to

the arc-arc collisional tectonics of the Hokkaido region, as the rupture of the main shock terminated at this high Vp region. We suggest that the plate interface geometry and the trench-parallel velocity heterogeneity in the landward plate are principal factors in controlling the rupture area of the main shock.

Keywords: The 2003 Tokachi-oki earthquake, subduction, ocean bottom seismometers, asperity, seismic tomography,

1. Introduction

Off the southeastern coast of Hokkaido Island in northern Japan, large interplate earthquakes have occurred repeatedly along the southernmost segment of the Kuril Trench, where the Pacific Plate subducts at a rate of 8-9 cm/year (DeMets, 1992) beneath the North American Plate (Fig. 1). During the past 60 years, five large interplate earthquakes have occurred in and around this region: the 1952 Tokachi-oki earthquake (Mw = 8.1, Kasahara, 1976), the 1968 Tokachi-oki earthquake (Mw = 8.5, Kanamori, 1971), the 1969 Shikotan earthquake (Mw = 8.2, Abe, 1973), the 1973 Nemuro-oki earthquake (Mw = 7.8, Shimazaki, 1974), and the 2003 Tokachi-oki earthquake (Mw = 8.0). The rupture areas were mainly estimated by the aftershock areas of each earthquake. Though the rupture areas of the former four earthquakes do not seem to overlap, the 1952 and 2003 Tokachi-oki earthquakes have the same areas of rupture. It is therefore considered that each large earthquake in the southern Kuril Trench has had a spatially characteristic source area.

From various seismological studies in northern Japan (e.g. Igarashi et al., 2003; Yamanaka and Kikuchi, 2004), it has recently become apparent that the recurrence of a large earthquake results from the repeated rupture of a spatially identical source area along the plate boundary. Two large interplate earthquakes have occurred in the Tokachi-oki area: March 4, 1952, and September 26, 2003. The epicenters of these two

earthquakes are less than 5km from each other. Yamanaka and Kikuchi (2003) estimated the slip distribution (seismogenic asperity) of the 2003 Tokachi-oki earthquake from teleseismic records, and compared the 2003 seismogenic asperity to that of the 1952 event, which was estimated from strong motion records. They suggested that the 2003 Tokachi-oki event was a recurrence of the 1952 event.

Controlled seismic source surveys using ocean bottom seismometers (OBSs) have been conducted in order to clarify the relation between large interplate earthquakes and seismic structure of this region (e.g., Iwasaki et al., 1989; Nakanishi et al., 2004). A tomographic study using micro-earthquakes recorded by OBSs off southern Hokkaido has also been performed (Murai et al., 2003), though the authors could not show any relation between the spatial variation of micro-seismicity and the velocity structure just above the seismogenic zone. Furthermore, recent studies suggest that fluids play an important role in the earthquake nucleation process, as fluids decrease the effective stress on a fault (Byerlee, 1993; Sibson, 1992). The spatial distribution of the ratios of P-wave velocity (Vp) to S-wave velocity (Vs) is considered to give information about the distribution of fluids. Therefore, information about the Vp structures and Vp/Vs ratios is needed for a better understanding of large earthquakes that occur as a result of stress-concentration on the plate boundary between the Kuril Island Arc and the Pacific Plate.

Additionally, revealing the structure around the southernmost Kuril Trench will

help us to better understand the tectonics of the Hokkaido region. At the southwestern end of the Kuril Trench, a collision between the Kuril Arc with the Northeastern Japan Arc is in progress, due to the oblique subduction of the Pacific Plate (Kimura, 1986). The Hidaka Mountains are considered to have become uplifted as the middle/lower crust of the Kuril Arc is obducted onto the North American Plate in the collision of the Kuril Arc with the Northeastern Japan Arc (e.g. Takanami, 1982; Iwasaki et al., 1998, 2004) (Fig 1). The Abashiri Tectonic Line and the Kushiro Submarine Canyon are located east of the Hidaka Mountains (Figure 1). From the axial directions of crustal folds in eastern Hokkaido, Sakurai et al. (1975) showed that, south of eastern Hokkaido, the Pacific Plate is structurally divided into two parts by the Kushiro Canyon. Based on the similarity of the tectonic pattern for both the east and west sides of the canyon, Kimura (1981a) showed that the Abashiri Tectonic Line extends to the Kushiro Canyon. Kimura (1981a) also suggested that the eastern Hokkaido region is divided into two structural units by the Abashiri Tectonic Line and the Kushiro Canyon. However, data concerning the detailed structure off southeastern Hokkaido that would support these interpretations at the crustal depth level has not yet been obtained.

Soon after the 2003 Tokachi-oki earthquake, aftershock observations using a dense OBS network were carried out to determine the precise aftershock distribution, and the detailed hypocenter distribution was estimated (Shinohara et al., 2004; Yamada et al., 2005). However, previous studies did not deploy a tomographic study toward

obtaining information about the velocity structure. For the present article, we carried out a simultaneous inversion using the aftershock data of the 2003 event obtained by the OBSs to estimate the Vp and Vp/Vs structure and precise hypocentral parameters. From the Vp and Vp/Vs models and hypocenter distribution, we infer a plate boundary geometry that includes the source region of the 2003 event. Finally, we discuss the plate boundary geometry and the detailed velocity structure of the overriding plate in relation to the size of the source region of the 2003 event.

2. Data

Four days after the occurrence of the 2003 Tokachi-oki earthquake, we started aftershock observations using pop-up type OBSs. Based on the aftershock distribution determined by land stations and a previous seismic refraction study (Iwasaki et al., 1989), it was decided to space the OBSs approximately 15 km apart near the Kuril Trench, and about 20 km apart closer to land (Fig. 1). During the aftershock observations, 9 OBSs were recovered in order to get an early aftershock distribution, and additional OBSs were deployed to monitor the spreading of the aftershock area toward the northeast (Shinohara et al., 2004). A total of 47 OBSs were deployed. A detailed account of the period of observation and the distribution of OBSs are described in Shinohara et al. (2004) and Yamada et al. (2005).

Each OBS was a free-fall and pop-up type with commandable releaser incorporating a three-component velocity sensor with natural frequency of 4.5 Hz. One broadband seismic sensor was also deployed. The locations of the OBSs on the sea floor were determined using acoustic ranging and ship GPS positions. The clock of each OBS was adjusted to the GPS time using the time difference measured just before and after the observation. Accurate timing was maintained within a few tens of milliseconds by a crystal oscillator in each OBS.

3. Hypocenter determination

The Japan Meteorological Agency (JMA) determined the hypocenters of 1159 events using land seismic network data over the period of our OBS observations. Using the P- and S-wave arrivals of the 1159 events listed in the JMA catalogue, we selected events that had more than 25 P and S arrival readings. As a result, 589 events remained for the hypocenter location.

We estimated the hypocenters of the aftershocks using a location program for finding a maximum likelihood solution using a Bayesian approach (Hirata and Matsu'ura, 1987). The velocity distribution for the location was modeled from a previous refraction survey conducted in the same region (Iwasaki et al., 1989). We used a simple one dimensional Vp structure, and we assumed a Vp/Vs of 1.73. The delay of arrival times by the sedimentary layer was also taken into account for the location. In general, seismic waves recorded by OBSs arrive later than those calculated using the average structure model due to unconsolidated sediments (e.g., Hino et al., 2000). We thus adjusted the calculated P- and S-wave arrivals using averaged differences between the observed and calculated travel times for each OBS (Shinohara et al., 2004, Table 1).

The epicenter distribution relocated by the OBS data is not uniform within the OBS network (Figure 2). The seismicity of aftershocks was low in the vicinity of the epicenter of the main shock and in the northeastern area. In contrast, there were many

aftershock epicenters near the center of the network and the northwestern area. These results are consistent with those of Yamada et al. (2005). In a vertical section, both aftershock distributions concentrate to form a landward dipping zone, above which they are more dispersed.

4. 3-D tomographic inversion using aftershock data of the 2003 Tokachi-oki earthquake

We estimated a 3-D velocity model using the SIMULPS14 algorithm (Haslinger and Kissling, 2001). The SIMULPS14 code originates from the simultaneous inversion of Vp, Vp/Vs, and hypocenter locations developed by Thurber (1983), Um and Thurber (1987), and Eberhart-Phillips (1986, 1990). Haslinger and Kissling (2001) improved the code to use a full 3-D shooting ray tracer. We solved for Vp and Vp/Vs using the P-wave arrival time data and the time differences between the S- and P-waves. Because reading errors of S-wave arrivals are generally larger than those of P-waves, the resolution of the Vs model obtained by the inversion is lower than that of the Vp model. The low resolution of the Vs model entails some difficulty in interpreting the Vp/Vs variations (Eberhart-Phillips and Reyners, 1997; Husen et al., 2000). Directly inverting the Vp/Vs model gives a better result, because the inversion of Vp/Vs can also use the high resolution data from the Vp model. Furthermore, the Vp/Vs ratio is directly related to Poisson's ratio, which is a key parameter in deriving petrophysical properties from seismic velocities.

A proper damping parameter reduces data variance without causing a large increase in solution variance (Eberhart-Phillips, 1986). For this reason, the damping value should be selected by estimating a trade-off curve between the data variance and solution variance. We used Vp and Vp/Vs damping values of 30 and 50, respectively.

191 The selected values greatly reduced the data variance with a moderate increase in the
192 solution variance.

193 Model resolution is assessed using a checkerboard resolution test (CRT)
194 (Sparkman and Nolet, 1988) that evaluates the spatial resolution of the data set. We also
195 examined the resolution of the results using the derivative weighted sum (DWS: relative
196 ray density in the vicinity of a model node), the diagonal element of the full resolution
197 matrix (RDE), and the spread function, which summarizes the information contained in
198 a single averaging vector or row of the full resolution matrix (Toomy and Fouliger,
199 1989; Michelini and McEvilly, 1991).

200 In the CRT, we used a 5 % velocity perturbation checkerboard. The CRT data
201 were inverted using the same method as for the real data. The results of the CRT (Figure
202 3) with a horizontal grid spacing of 20km show a fairly good resolution at depths of 15,
203 20, and 25 km for both Vp and Vp/Vs under the OBS network. In these regions, the
204 recovered magnitudes of the velocity anomaly were 4 % for Vp and 3.5 % for Vp/Vs on
205 average. At a depth of 10km, perturbations of Vp and Vp/Vs were detected in the central
206 part of the OBS network. We therefore decided to use a grid spacing of 20 km in the
207 horizontal direction for the tomographic inversion of the OBS data set (Figure 2). For
208 the vertical direction we used a grid spacing of 5 km for depths between 0 km and 25
209 km. In the region deeper than 25 km, a grid spacing of 10 km was used for the Vp and
210 Vp/Vs model. The starting 1-D velocity model for the inversion (Table 2) was based on

211 the refraction survey (Iwasaki et al., 1989), and an initial Vp/Vs ratio of 1.73 was
212 assumed.

213 DWS, RDE and the spread function are important parameters for estimating the
214 resolution of the results. These parameters were calculated for the last iteration of the
215 inversion. These values and the results of the CRT were considered to indicate regions
216 of high Vp and Vp/Vs resolution. Finally, we considered regions with a spread function
217 of less than 0.5, RDE values larger than 0.5, and DWS values larger than 1000 to be of
218 high resolution.

219

220

5. Results

We used 589 events with 12,134 P-wave arrivals and 10,802 S-P times for the 3-D inversion, and phase weighting was applied based on estimated picking errors. We estimated a picking error of 0.1 s for P-wave arrivals and 0.2 s for S-P times. After five iterations, the combined root-mean square (rms) was 0.22 s, with data variances of 0.0283 s^2 for P-wave arrivals and 0.0772 s^2 for S-P times, and a model variance of 0.08012 km^2/s^2 for P-wave arrivals and 0.00387 km^2/s^2 for S-P times. The initial combined rms was 0.33 s. The initial data variances for P-wave arrivals and S-P times were 0.0818 s^2 and 0.1553 s^2, respectively. The initial model variances for P-wave arrivals and S-P times were 0.00520 km^2/s^2 and 0.00029 km^2/s^2, respectively.

Hypocenters were also relocated using tomographic inversion. The means of the absolute location changes of the hypocenters between the initial locations and the final results are 1.11 km north, 1.65 km east, and 0.13 km in depth. Figure 4 shows the differences between the initial and relocated hypocenters. The relocated hypocenters give a clear image of a landward dipping plane that extends from 15 to 45 km in depth.

To interpret the results of the 3-D inversion, we plotted a series of vertical depth sections of the final 3-D Vp model perpendicular to and parallel to the strike of the trench (Figure 5). Figure 6 shows vertical cross sections perpendicular to the trench for the Vp and Vp/Vs results. The vertical sections parallel to the trench for the Vp result

240 are also shown in Figure 7. Regions with low resolution are shaded, in accordance with
241 the resolution analysis described in the previous section. Abundant aftershock data from
242 the dense OBS network enabled the imaging of a high Vp anomaly (7-8 km/s) dipping
243 landward in all the profiles (Figure 6). The dipping high Vp region corresponds to the
244 dipping plane defined by the relocated hypocenters (Figure 6).
245

245 ## 6. Discussion

246

247 ### 6-1 Bending of the subducting plate and rupture propagation

248

249 A high Vp anomaly is to be expected within the subducting oceanic plate, because
250 the Pacific Plate should be cold due to its old age. Based on a comparison with the
251 previous refraction survey of Iwasaki et al. (1989), the high Vp anomaly appears to
252 correspond to the subducting oceanic crust and uppermost mantle. A high Vp/Vs
253 anomaly is found at the region of the high Vp anomaly. Christensen (1996) showed that
254 rocks mainly composing an oceanic crust have a Vp/Vs greater than 1.8. Therefore the
255 high Vp/Vs of the crust in our results is considered to be reasonable. The existence of
256 the high Vp/Vs anomaly in the region of the high Vp anomaly is considered to be
257 further evidence of the crust of the subducting Pacific Plate.

258 Figure 8 shows the spatial distribution and vertical section of the relocated
259 hypocenters. The aftershocks in the lower part of the high activity region form a
260 landward dipping plane. The relocated hypocenters can be compared with the velocity
261 structure estimated by Iwasaki et al. (1989). The plane formed by the aftershock
262 locations in the lower part of the high activity region corresponds to the plate boundary
263 estimated from the velocity structure. The JMA determined the CMT solutions of the
264 aftershocks (Figure 8). Most of the hypocenters in the lower part of the high seismicity

region are indicative of thrust type events. Yamada et al. (2005) determined the focal mechanisms of aftershocks around the lower part of the high seismicity region using the first motions of P-wave arrivals. They are mainly characterized by a thrust type mechanism. Thus the lower boundary of the high seismicity region indicates the plate boundary between the subducted plate and the overriding island arc crust.

Yamada et al. (2005) suggested that a change of the dip angle of the plate boundary occurs in the study area. Our relocated hypocenters are estimated to have higher resolution than those of Yamada et al. (2005), because we use the simultaneous inversion technique to estimate 3-D velocity structures and hypocentral parameters. The bending of the subducting Pacific Plate is recognized from our relocated hypocenters in all cross sections of Figure 6. The dip angle of the plate boundary is less than 5˚ at distances of less than 90 km from the Kuril Trench axis, but increases abruptly to an angle greater than 16˚ (Figure 8). In other words, the precise hypocenters relocated in this study suggest that the plate boundary becomes steep at a distance of approximately 90 km from the Kuril Trench axis. The previous reflection study clearly imaged reflections at depths of 24-25 km with a landward dip angle of 16˚ (Tsuru et al., 2005). The reflections are positioned at distances of 15-20 km landward from the epicenter of the 2003 Tokachi-oki earthquake.

Several studies have found that the bending of the subducting plate occurs in the Northern Japan Trench, and have discussed the relation between this bending and

285 rupture propagation. Ito et al. (2005), who conducted an onshore-offshore wide-angle
286 and reflection survey, point out that the dip angle of the subducting plate changes
287 sharply near the eastern edge of rupture area of the 1981 event (Mw = 7.1), in the region
288 off Miyagi. Fujie et al. (2006) also found sharp plate bending in the region off Iwate,
289 and they suggest that the coseismic rupture of a large interplate earthquake would not
290 propagate beyond that bending. The seismogenic asperity of the 2003 Tokachi-oki
291 earthquake (Yamanaka and Kikuchi, 2003) is projected on the vertical sections of our
292 tomographic images (Figure 6). The bending positions correspond to an updip limit of
293 the seismogenic asperity during the 2003 Tokachi-oki earthquake by Yamanaka and
294 Kikuchi (2004). Figure 8 shows the comparison between the spatial distribution of the
295 seismogenic asperity of the 2003 Tokachi-oki earthquake and the plate bending
296 positions. From these results, we conclude that the coseismic rupture of the 2003 event
297 occurred on the plate boundary with a steep dip angle, and did not propagate beyond the
298 sharply bending region.

299 Yamanaka and Kikuchi (2003) estimated the slip distribution of the 2003
300 Tokachi-oki earthquake using seismograms from the global seismic network, and they
301 indicated that the rupture had propagated northward into the deeper zone. A large slip
302 region (seismogenic asperity) estimated by Yamanaka and Kikuchi (2003) is
303 comparable with that of Yagi (2004), which was estimated using both teleseismic body
304 waves and strong ground motion records in Japan. Yamanaka and Kikuchi (2003) also

estimated the seismogenic asperity region of the 1952 Tokachi-oki earthquake from strong ground motion records obtained in Japan, and they concluded that the 1952 event and the 2003 event have the same seismogenic asperity. Furthermore, distributions of seismic intensity for the 1952 event and the 2003 event on mainland Hokkaido are similar (Hamada et al., 2004). This also indicates that the locations of the seismogenic asperities of the 1952 and the 2003 events are identical. However, the slip distributions (tsunamigenic asperities) of the 1952 and 2003 Tokachi-oki earthquakes, estimated from a tsunami waveform inversion, are different. For the 2003 event, the tsunamigenic asperity area corresponds to the seismogenic asperity area (Tanioka et al., 2004a). Conversely, the tsunami data evinces a large slip in the southeast of the seismogenic asperity of the 1952 Tokachi-oki event (Hirata et al., 2003). The largest slip in the 1952 tsunamigenic asperity is located on the plate boundary with a dip angle less than 5˚ (Figure 8). Additionally, large tsunami heights were observed at the 1952 event on the eastern coasts of Hokkaido, where the tsunami heights at the 2003 event were comparatively small (Tanioka et al., 2004b). As a result, both the 1952 event and the 2003 event are considered to be ruptures of the same region on the plate boundary with a dip angle greater than 16˚. The 1952 Tokachi-oki earthquake is estimated to have simultaneously generated a slow slip on the plate boundary with a dip angle less than 5˚. In conclusion, the rupture of the 1952 events propagated beyond the area of plate bending, and the rupture velocity on a plate boundary with a dip angle less than 5˚ may

325 be slow.

326

327 6-2 Possibility of fluid flow associated with the 2003 Tokachi-oki earthquake

328

329 Several recent studies have proposed that fluids play an important role in
330 earthquake nucleation, as fluids lower the effective stress on a fault (Byerlee, 1993;
331 Sibson, 1992). Changes of fluid distribution during the occurrence of large earthquakes
332 have also been inferred in other studies (Magee and Zobak, 1993; Husen and Kissling,
333 2001). Furthermore, spatio-temporal variations in reflectivity were found near the
334 source area of the 2003 Tokachi-oki earthquake (Tsuru et al., 2005).

335 A high anomaly with a Vp/Vs greater than 1.88 was found at depths of 15-20 km
336 and at a distance of 20-30 km landward from the epicenter of the 2003 Tokachi-oki
337 earthquake (Figure 6). The anomaly occurs about 10 km above the plate boundary.
338 Figure 9 shows the distribution of Vp and Vp/Vs on the depth slices. High Vp/Vs
339 anomalies corresponding to the subducting oceanic crust is clearly seen near the plate
340 boundary (dashed lines). However, a Vp/Vs anomaly is also found to the north of the
341 epicenter of the 2003 Tokachi-oki earthquake in the 15 and 20 km depth sections. The
342 high Vp/Vs anomaly in the northern region is positioned in the crust of the landward
343 plate, and is about 20 km wide. The high Vp/Vs region in the landward crust extends
344 approximately 10 km upward from the plate boundary. The high Vp/Vs anomaly in the

345 northern region is distinguished from that of the subducting oceanic crust, and
346 corresponds to the largest amount of slip in the 2003 seismogenic asperity (Yamanaka
347 and Kikuchi, 2003). The Vp corresponding to the high Vp/Vs region in the landward
348 crust is about 7.0 km/s (Figure 9, upper). The P-wave velocity of 7 km/s is considered to
349 be related to a lower crust composed of mafic (gabbroic) rocks. Furthermore, the Vp/Vs
350 greater than 1.88 in our results is larger than that of dry gabbro, which indicates the
351 possibility that the presence of a fluid has increased the Vp/Vs value.

352 Husen and Kissling (2001) found regions with high Vp/Vs ratios in the subducting
353 Nazca Plate and above the rupture region of the 1995 Antofagasta earthquake (Mw =
354 8.0). They suggested a permeability-seal breaking model to explain the time evolution
355 of changes of Vp/Vs within the rupture area. The permeability-seal is considered to be
356 formed by the high stress along the plate interface (Husen and Kissling, 2001). This
357 means that a high Vp/Vs region above a plate interface where a subducting plate and a
358 landward plate were strongly coupled appears after large earthquakes. Although we
359 could not detect any temporal evolution of the Vp/Vs ratio for the 2003 Tokachi-oki
360 earthquake, it is possible that the high Vp/Vs anomaly is caused by fluid flowing into
361 the overlying island arc crust.

362

363 6-3 Correlation between the source region of the 2003 Tokachi-oki earthquake and
364 trench-parallel heterogeneity in the island arc crust

365

366 A thick layer with Vp greater than 7 km/s was detected above the plate boundary
367 (Figure 7). P-wave velocities in the island arc crust increase gradually from 5.7-6.6 in
368 the western part to 6.5-7.3 km/s in the eastern part. Such a high Vp layer in the island
369 arc crust was also inferred by previous studies (Iwasaki et al., 1989; Nakanishi et al.,
370 2004). These collected results concur that the P-wave velocities in the crust near the
371 Kushiro Canyon are larger than those above the seismogenic asperity area of the 2003
372 event.

373 Kimura (1981b, 1986) indicated that the Kuril fore-arc sliver has moved
374 southwestward since the Miocene, and collided with the Northeastern Japan Arc due to
375 the oblique subduction of the Pacific Plate. We interpret the high velocity anomaly
376 obtained from our 3-D inversion as a structural boundary related to this arc-arc collision
377 (Kimura, 1981a). The aftershock distribution of the 2003 Tokachi-oki earthquake shows
378 that many aftershocks occurred in the island arc crust, and that most of the aftershocks
379 in the landward crust have a focal strike-slip mechanism (Yamada et al., 2005). We infer
380 that strain in the landward crust had been accumulating due to the motion of the Kuril
381 forearc sliver until the 2003 event. The stress in the crust was released by the occurrence
382 of the 2003 Tokachi-oki earthquake, which caused many aftershocks in the island arc
383 crust. However, no aftershocks of the 2003 Tokachi-oki earthquake occurred on the
384 eastern side of the Kushiro Canyon (Watanabe et al., 2006).

385 The northeastern boundary of the seismogenic asperity of the 2003 Tokachi-oki
386 earthquake corresponds to the structural boundary which is seen in Profiles 6 and 7 in
387 Figure 7. From the Nafe-Drake curve (e.g. Ludwig et al., 1970), which is an empirical
388 relationship between density and seismic velocity, it is seen that seismic wave speeds in
389 the island arc crust in the Tokachi-oki region are indicative of low density material (2.7
390 * 10^3 kg/m^3). Relatively high density material (2.9 * 10^3 kg/m^3) is expected in the
391 northeastern region. Figure 10 shows a comparison between the free-air gravity
392 anomaly (FAA) (Smith and Sandwell, 1997) and the seismogenic asperity of the 2003
393 Tokachi-oki earthquake (Yamanaka and Kikuchi, 2003). Along Profile 6 of our study,
394 the regional seafloor topography is relatively smooth, and the water depth increases to
395 the northeast (Figure 10b). The FAA is generally consistent with bathymetry. However,
396 the low FAA appears in the region of the 2003 event seismogenic asperity (Figure 10c).
397 This indicates that the landward crust above the rupture area of the 2003 Tokachi-oki
398 earthquake is of low density. Wells et al. (2003) compared areas of high coseismic slip
399 for large earthquakes to the overlying plate structure estimated by satellite gravity,
400 bathymetry, and marine geophysical studies. They found that most of seismic moment
401 during the 1952 Tokachi-oki event was released beneath the prominent free-air gravity
402 low area. Temperature, fluid pressures, and stress are considered to be partly controlled
403 by the thickness and density of the landward plate. They inferred that variations in
404 crustal thickness and density of the landward crust along the trench affected the

405 coseismic slip for large earthquakes. Considering these results, a crustal seismic
406 structure in the overriding plate may affect the strength of a seismic coupling, and the
407 size of the rupture area of the 2003 Tokachi-oki earthquake should be controlled by the
408 structure of the island arc crust.
409
410

7. Conclusions

In the interest of estimating the 3-D velocity structure of the source area of the 2003 Tokachi-oki earthquake (Mw=8.0) off southern Hokkaido, Japan, we carried out seismic tomographic analysis using a large number of P- and S-wave arrivals from aftershocks recorded by OBSs. The hypocenters were also relocated simultaneously. The subducting plate beneath the OBS network was clearly imaged as a northwest dipping zone with a high Vp. The distribution of aftershocks relocated by the simultaneous inversion shows the shape of the subducting Pacific Plate. The dip angle of the plate boundary is less than 5˚ near the Kuril Trench, and increases abruptly to 16˚ approximately 90 km from the trench axis. The position of the plate bending coincides with the southeastern edge of the rupture area of the 2003 event. A high Vp/Vs anomaly is found northwest of the focus of the 2003 event, and extends about 10 km upward from the plate interface. The high Vp/Vs anomaly is positioned above the largest slip area, and may relate to fluid flow during the main shock. Lateral velocity variations parallel to the trench were found. A thick layer with Vp greater than 7 km/s is recognized in the landward crust in the eastern part of the study area. This high Vp region is interpreted as a structural unit related to the arc-arc collision on Hokkaido. The rupture of the 2003 main shock terminated at the edge of the high Vp region. Gravity data and our results show that the landward crust just above the rupture area of the 2003

event has low density. Consequently, we suggest that the plate interface geometry and the trench-parallel velocity heterogeneity are among the factors controlling the rupture of the main shock.

434 Acknowledgements

435

436 We wish to express thanks to the captains and crews of M/V Shinryu-maru, R/V
437 Natsushima, R/V Kofu-maru, and M/V Shintatsu-maru for their cooperation during
438 deployment and recovery of the OBSs, and all who helped with preparation of the OBS
439 observation. We thank Dr. Rolf Mjelde for his valuable comments, and Dr. Alan. T.
440 Linde for improvement of the text. Valuable comments from two anonymous reviewers
441 helped us to improve the manuscript. This study is partly supported by the Special
442 Coordination Funds for the Promotion of Science and Technology (MEXT, Japan),
443 entitled Urgent Research for the 2003 Tokachi-oki Earthquake. We used Generic
444 Mapping Tools (Wessel and Smith, 1995) and TOMO2GMT (available from Dr.
445 Stephan Husen) to make most of the figures for this article.

446

446 References

447

448 Abe, K., 1973. Tsunami and mechanism of great earthquakes. Phys. Earth Planet. Int. 7,
449 143-153.
450 Byerlee, J., 1993. Model for episodic flow of high-pressure water in fault zones before
451 earthquake. Geology, 21, 303-306.
452 Christensen, N.I., 1996. Poisson's ratio and crustal seismology. J. Geophys. Res., 101,
453 3,139-3,156.
454 DeMets, C., 1992. Oblique convergence and deformation along the Kuril and Japan
455 trenches. J. Geophys. Res., 97, 17,615-17,625.
456 Eberhart-Phillips, D., 1986. Three-dimensional velocity structure in northern California
457 Coast Range from inversion of local earthquake arrival times. Bull. Seismo. Soc.
458 Am., 76, 1025-1052.
459 Eberhart-Phillips, D., 1990. Three-dimensional P and S velocity structure in the
460 Coalinga region, California. J. Geophys. Res., 95, 15,343-15,363.
461 Eberhart Phillips, D, and Reyners, M., 1997. Plate interface properties in the Northeast
462 Hikurangi subduction zone, New Zealand, from converted seismic waves.
463 Geophys. Res. Lett., 26, 2,565-2,568.
464 Fujie, G., Ito, A., Kodaira, S., Takahashi, N., Kaneda, Y., 2006. Confirming sharp
465 bending of the Pacific plate in the northern Japan trench subduction zone by

applying a travel time mapping method. Phys. Earth Planet. Int., 157, 72-85.

Hamada, N., Suzuki, Y., 2004. Re-examination of aftershocks of the 1952 Tokachi-oki earthquake and a comparison with those of the 2003 Tokachi-oki earthquake. Earth Planet Space, 56, 341-345

Haslinger, F., Kissling, E., 2001. Investigating effects of 3-D ray tracing methods in local earthquake tomography. Phys. Earth Planet. Int. 123, 103-114.

Hino, R., Ito, S., Shiobara, H., Shimamura, H., Kanazawa, T., Sato, T., Kasahara, J., Hasegawa, A., 2000. Aftershock distribution of the 1994 Sanriku-oki earthquake (Mw 7.7) revealed by ocean bottom seismographic observation. J. Geophys. Res., 105, 21,697-21,710.

Hirata, K., Geist, E., Satake, K., Tanioka, Y., Yamaki, S., 2003. Slip distribution of the 1952 Tokachi-oki earthquake (M 8.1) along the Kuril Trench deduced from tsunami waveform inversion. J. Geogphys. Res., 108, 2196, doi:10.1029/2002JB001976.

Hirata, N., Matsu'ura, M., 1987. Maximum-likelihood estimation of hypocenter with origin time eliminated using nonlinear inversion technique. Phys. Earth Planet. Int.,47, 51-61.

Husen, S., Kissling, E., Flueh, E.R., 2000. Local earthquake tomography of shallow subduction in north Chile: a combined onshore and offshore study. J. Geophys. Res., 105, 28,183-38198.

Husen, S., Kissling, E., 2001. Postseismic fluid flow after the large subduction earthquake of Antofagasta, Chile. Geology, 29, 847-850.

Igarashi, T., Matsuzawa, T., Hasegawa, A., 2003. Repeating earthquakes and interplate aseismic slip distribution in the northeastern Japan subduction zone. J. Geophys. Res., 108(B5), 2249, doi:10.1029/2002JB001920.

Ito, A., Fujie, G., Miura, S., Kodaira, S., Kaneda, Y., 2005. Bending of the subducting oceanic plate and its implication for rupture propagation of large interplate earthquakes off Miyagi, Japan, in the Japan Trench subduction zone. Geophys. Res. Lett, Vol. 32, L05310, doi:10.1029/2004GL022307.

Iwasaki, T., Shiobara, H., Nishizawa, A., Kanazawa, T., Suyehiro, K., Hirata, K., Urabe, T., Shimamura, H., 1989. A detailed subduction structure in the Kuril trench deduced from ocean bottom seismographic refraction studies. Tectonophysics, 165, 315-336.

Iwasaki, T., Ozel, Z., Moriya, T., Kobayashi, A., Nishiwaki, M., Tsutsui, T., Iidaka, T., 1998, Lateral structural variation across a collision zone in central Hokkaido, Japan, as revealed by wide-angle seismic experiments. Geophys. J. Int. 132, 435-457.

Iwasaki, T., Adachi, K., Moriya, T., Miyamachi, H., Matsushima, T., Miyashita, K., Takeda, T., Taira, T., Yamada, T., Ohtake, K., 2004. Upper and middle crustal deformation of an arc-arc collision across Hokkaido, Japan, inferred from seismic

refraction/wide-angle reflection experiments. Tectonophysics 388, 59-73

Kasahara, M., 1976. Vertical crustal movement around Cape Erimo, southern part of Hokkaido and a brief of the recent crustal movement of Hokkaido region (in Japanese). paper presents at Symposium on Subterranean Structure in and Around Hokkaido and its Tectonic Implication Inst, of Seismol. And Volcanol., Hokkaido Univ., Sapporo, Japan.

Kanamori, H., 1971. Focal mechanism of the Tokachi-oki earthquake of May 16, 1968: Contortion of the lithosphere at a junction of two trenches. Tectonophysics, 12, 1-13.

Kimura, G., 1981a. Abashiri Tectonic Line - with special reference to the tectonic significance of the southwestern margin of the Kuril Arc. Jour. Fac. Sci., Hokkaido Univ., Sec. IV, 20, 95-111.

Kimura, G., 1981b. Tectonics at the southwestern margin of the Kuril Arc and tectonics stress field. Journal of the Geological Society of Japan, 87, 757-68.

Kimura, G., 1986. Oblique subduction and collision: forearc tectonics of the Kuril arc. Geology 14, 404-407.

Ludwig, W. J., Nafe, E., Drake, C.L, 1970. Seismic refraction. In A. E. Maxwell, ed., The Sea, Vol. 4, Part 1. New York: Wiley-Interscience, pp. 53-84.

Magee, M., Zobak, M.D., 1993. Evidence for a weak interplate thrust fault along the northern Japan subduction zone and implications for the mechanics of thrust

faulting and fluid expulsion. Geology, 21, 809-812.

Michelini, A., McEvilly, T. V., 1991. Seismological studies at Parkfield: I. Simultaneous inversion for velocity structure and hypocenters using cubic b-splines parameterization. Bull. Seismo. Soc. Am., 81, 524-552.

Murai, Y., Akiyama, S., Katsumata, K., Takanami, T., Yamashina, T., Watanabe, T., Cho, I., Tanaka, M., Kuwano, A., Wada, N., Shimamura, H., Furuya, I, Zhao, D., Sanda, R., 2003. Delamination structure imaged in the source area of the 1982 Urakawa-oki earthquake. Geophys. Res. Lett., Vol. 30, NO. 9, 1490, doi:10.1029/2002GL016459.

Nakanishi, A., Smith, A.J., Miura, S., Tsuru, T., Kodaira, S., Obana, K., 2004. Structural factors controlling the coseismic rupture zone of the 1973 Nemuro-oki earthquake, the southern Kuril Trench seismogenic zone. J. Geophys. Res., Vol. 109, B05305, doi:10.1029/2003JB002574.

Sakurai, M., Nagai, T., Tozawa, M., Ikeda, K., 1975. Submarine geological structures and crustal movements of the continental margin off Kushiro, Hokkaido. Report of invest. Nemurooki Earthquake. 17, June, 1973, part I: 10-17. (in Japanese with English abstract).

Shimazaki, K., 1974. Nemuro-oki earthquake of June 17, 1973: A lithospheric rebound at the upper half of the interface. Phys. Earth Planet. Int., 49, 54-77.

Shinohara, M., Yamada, T., Kanazawa, T., Hirata, N., Kaneda, Y., Takanami, T., Mikada,

546 H., Suyehiro, K., Sakai, S., Watanabe, T., Uehira, K., Murai, Y., Takahashi, N.,
547 Nishino, M., Mochizuki, K., Sato, T., Araki, E., Hino, R., Uhira, K., Shiobara, H.,
548 Shimizu, H., 2004. Aftershock observation of the 2003 Tokachi-oki earthquake by
549 using dense ocean bottom seismometer network. Earth Planets Space, 56,
550 295-300.
551 Sibson, R.H., 1992. Implications of fault-valve behavior for rupture nucleation and
552 recurrence. Tectonophysics, 211, 283-293.
553 Smith, W.H.F., Sandwell, D.T., 1997. Global seafloor topography from satellite
554 altimetry and ship depth soundings. Science 277, 1957-1962.
555 Sparkman, W., Nolet, G., 1988. Imaging algorithm, accuracy and resolution in delay
556 time tomography, in Mathematical Geophysics, edited by N. Vlarr et al., pp.
557 155-187, Springer, New York.
558 Takanami, T., 1982. Three-dimensional seismic structure of the crust and upper mantle
559 beneath the orogenic belt in southern Hokkaido, Japan. J. Phys. Earth, 30, 87-104.
560 Tanioka, Y., Hirata, K., Hino, R., Kanazawa, T., 2004a. Slip distribution of the 2003
561 Tokachi-oki earthquake estimated from tsunami waveform inversion. Earth
562 Planets Space, 56, 373-376.
563 Tanioka, Y., Nishimura, Y., Hirakawa, K., Imamura, F., Abe, I., Abe, K., Shindou, H.,
564 Matsutomi, H., Takahashi, T., Imai, K., Harada, K., Namegawa, Y., Hasegawa, Y.,
565 Hayashi, Y., Nanayama, F., Kamataki, T., Kawata, Y., Fukawasa, S., Koshima, S.,

566 Hada, Y., Azumai, Y., Hirata, K., Kamikawa, A., Yoshikawa, A., Shiga, T.,
567 Kobayashi, M., Masaka, S., 2004b. Tsunami run-up heights of the 2003
568 Tokachi-oki earthquake. Earth Planets Space, 56, 359-365.
569 Thurber, C.H., 1983. Earthquake locations and three-dimensional crustal structure in the
570 Coyote lake area, central California. J. Geophys. Res., 88, 8226-8236.
571 Toomy, D.R., Foulger, G.R., 1989. Tomographic inversion of local earthquake data from
572 the Hengill-Grensdalur central volcano complex, Iceland. J. Geophys. Res., 94,
573 17,497-17,510.
574 Tsuru, T., Park, J.-O., Kido, Y., Ito, A., Kaneda, Y., Yamada, T., Shinohara, M., 2005.
575 Did expanded porous patches guide rupture propagation in 2003 Tokachi-oki
576 earthquake? Geophys. Res. Lett, Vol. 32, L20310, doi:10.1029/2005GL023753.
577 Um, J., Thurber, C.H., 1987, A fast algorithm for two-point seismic ray tracing. Bull.
578 Seismo. Soc. Am. 77,972-986.
579 Watanabe, T., Takahashi, H., Ichiyanagi, M., Okayama, M., Takada, M., Otsuka, M.,
580 Hirata, K., Morita, S., Kasahara, M., Mikada, H., 2006. Seismological monitoring
581 on the 2003 Tokachi-oki earthquake, derived from off Kushiro permanent cabled
582 OBSs and land based observations. Tectonophysics, 426, 107-118.
583 Wells, R.E., Blakely, R.J., Sugiyama, Y., Scholl, D.W., Dinterman, P.A., 2003.
584 Basin-centered asperities in great subduction zone earthquakes: A link between
585 slip, subsidence, and subduction erosion? J. Geophys. Res. 108, 2507,

586 doi:10.1029/2002JB002072.
587 Yagi, Y., 2004. Source rupture process of the 2003 Tokachi-oki earthquake determined
588 by joint inversion of teleseismic body wave and strong ground motion data. Earth
589 Planets Space, 56, 311-316.
590 Yamada, T., Shinohara, M., Kanazawa, T., Hirata, N., Kaneda, Y., Takanami, T., Mikada,
591 H., Suyehiro, K., Sakai, S., Watanabe, T., Uehira, K., Murai, Y., Takahashi, N.,
592 Nishino, M., Mochizuki, K., Sato, T., Araki, E., Hino, R., Uhira, K., Shiobara, H.,
593 Shimizu, H., 2005. Aftershock distribution of the 2003 Tokachi-oki earthquake
594 derived from high-dense network of ocean bottom seismographs (in Japanese).
595 Zisin, 57,281-290.
596 Yamanaka, Y., Kikuchi, M., 2003. Source process of the recurrent Tokachi-oki
597 earthquake on September 26, 2003, inferred from teleseismic body waves. Earth
598 Planets Space, 55, e21-e24.
599 Yamanaka, Y., Kikuchi, M., 2004. Asperity map along the subduction zone in
600 northeastern Japan inferred from regional seismic data. J. Geophys. Res., 76,
601 329-336.
602
603
604
605

605 Figure captions

606

607 Figure 1. (Upper): Tectonic setting around Hokkaido, Japan, and source regions of the
608 large earthquakes along the southern Kuril Trench. Locations of the Abashiri Tectonic
609 Line and the Hidaka Mountains are indicated. The rectangle indicates the study area.
610 (Lower): Distribution of OBS stations (triangles) used in this study, and the epicenter of
611 the 2003 Tokachi-oki earthquake (star) with bathymetry. The thick contours show the
612 amount of fault slip for the 2003 main shock as determined by seismic waves
613 (Yamanaka and Kikuchi, 2003). The contour interval is 0.5 m. The thick line indicates
614 the profile of a previous seismic survey using OBSs (Iwasaki et al., 1989). Location of
615 the Kushiro Canyon is indicated by an arrow.

616

617 Figure 2. (Upper): Aftershock distribution located with a 1-D velocity structure using
618 the OBS network data. The number of events is 589. Triangles denote the positions of
619 the OBSs. The star and the gray circles represent the epicenters of the 2003 main shock
620 and aftershocks, respectively. Crosses show the horizontal positions of the grid for 3-D
621 Vp and Vp/Vs tomographic inversion. (Lower): Depth distribution of the aftershocks
622 projected onto the vertical cross section along A-A'.

623

624 Figure 3. Results of the Checkerboard Resolution Test (CRT) with a grid spacing of 20

625 km. Upper and lower rows indicate the CRT results for Vp and Vp/Vs, respectively. The
626 depth of each section is shown in the upper left corner. White and black circles represent
627 high and low anomalies, respectively.
628
629 Figure 4. (Upper): Comparison between the initial hypocenters (gray circles) and those
630 relocated by the 3-D inversion (black circles). The triangles and star indicate the
631 positions of OBSs and the epicenter of the 2003 Tokachi-oki earthquake, respectively.
632 (Lower): Hypocenters projected onto the vertical cross section along A-A'.
633
634 Figure 5. Positions of vertical profiles (solid black line) with horizontal grid positions
635 for the 3-D tomographic inversion. The star and triangles represent the epicenter of the
636 2003 event and the positions of seismic stations, respectively.
637
638 Figure 6. Vertical depth sections for absolute Vp (left) and Vp/Vs (right) along the dip
639 of the Pacific Plate. Distance in the horizontal axis is measured from the trench axis.
640 Locations of the depth sections are shown by thick lines in Figure 5. Stars indicate the
641 hypocenter of the main shock. The source depth of the main shock was estimated by
642 Shinohara et al. (2004). The areas with shaded colors have a low resolution of velocity.
643 Hypocenters at a distance of less than 20km from the profile are plotted in each section.
644 The projected regions with a slip greater than 0.5m during the main shock (Yamanaka

645 and Kikuchi, 2003) are shown by dashed lines under each vertical depth section.

646

647 Figure 7. Same as Figure 6, but parallel to the trench axis. Distance in the horizontal
648 axis is measured from the southwestern edge of each profile.

649

650 Figure 8. (Upper): Distribution of 589 relocated aftershocks determined beneath the
651 OBS network. The yellow star and the gray circles represent the epicenters of the 2003
652 event and of the relocated hypocenters, respectively. Triangles denote positions of the
653 OBSs. CMT solutions determined by JMA are shown at the lower left. Lower
654 hemisphere projection is used. The position of the plate bending is indicated by a
655 dashed line. The high P-wave velocity zone (HVZ) in the island arc crust is surrounded
656 by a dashed curve. Slip distribution (seismogenic asperity) of the 2003 Tokachi-oki
657 earthquake (Yamanaka and Kikuchi, 2003) is shown (thin contours). The tsunamigenic
658 asperity of 1952 Tokachi-oki earthquake (Hirata et al., 2003) is also indicated (gray
659 regions). Note that the position of the plate bending and the boundary of the HVZ
660 correspond to the boundary of the seismogenic asperity of the 2003 Tokachi-oki event.
661 (Lower): Distribution of the relocated hypocenters projected on the vertical cross
662 section along A-A'. Numerals indicate aftershocks for which the CMT solutions are
663 plotted in the upper figure. The plate boundary estimated by the aftershock distribution
664 is indicated by the thick red broken line. High seismicity was observed within the

665 landward plate.

666

667 Figure 9. Distribution of Vp (upper) and Vp/Vs (lower) in the final results. The
668 horizontal sections at depths of 10 km, 15 km, 20 km, and 25 km are shown. The
669 P-wave velocity and Vp/Vs ratios are color coded. Regions of poor resolution are
670 shaded gray. Triangles represent the positions of seismic stations. The contours indicate
671 the fault slip distribution of the 2003 Tokachi-oki earthquake (Yamanaka and Kikuchi,
672 2003). The contour interval is 0.5 m. Dashed lines in the Vp/Vs distributions (lower) at
673 depths of 15, 20, and 25 km indicate the position of the plate boundary at each depth.
674 High Vp/Vs anomalies within the landward crust are shown by ellipses.

675

676 Figure 10. The relation among topography, free-air gravity anomaly, and slip
677 distribution. (a) Free-air gravity anomaly with bathymetry (after Smith and Sandwell,
678 1997). The amplitude of the free-air gravity anomaly is color coded. The yellow star and
679 the green triangles show the epicenter of the 2003 Tokachi-oki earthquake and the
680 positions of OBSs, respectively. Contours drawn by dashed curves show the fault slip
681 distribution (Yamanaka and Kikuchi, 2003). The contour interval is 0.5 m. The positions
682 of the vertical sections used in this study are indicated by black lines. (b) Variation in
683 seafloor topography along Profile 6. (c) Variation in the free-air gravity anomaly along
684 Profile 6. (d) Variation in slip distribution along Profile 6.

685

686 Table 1. Root mean square (RMS) of the averaged residual between observed and
687 calculated travel times during the hypocenter location using 1-D velocity structure. SC:
688 station correction.

689 Table 2. Initial 1-D velocity distribution of Vp and Vp/Vs velocity models used for the
690 3-D tomographic inversion. The model is derived from a previous refraction study that
691 used OBSs (Iwasaki et al., 1989).

692

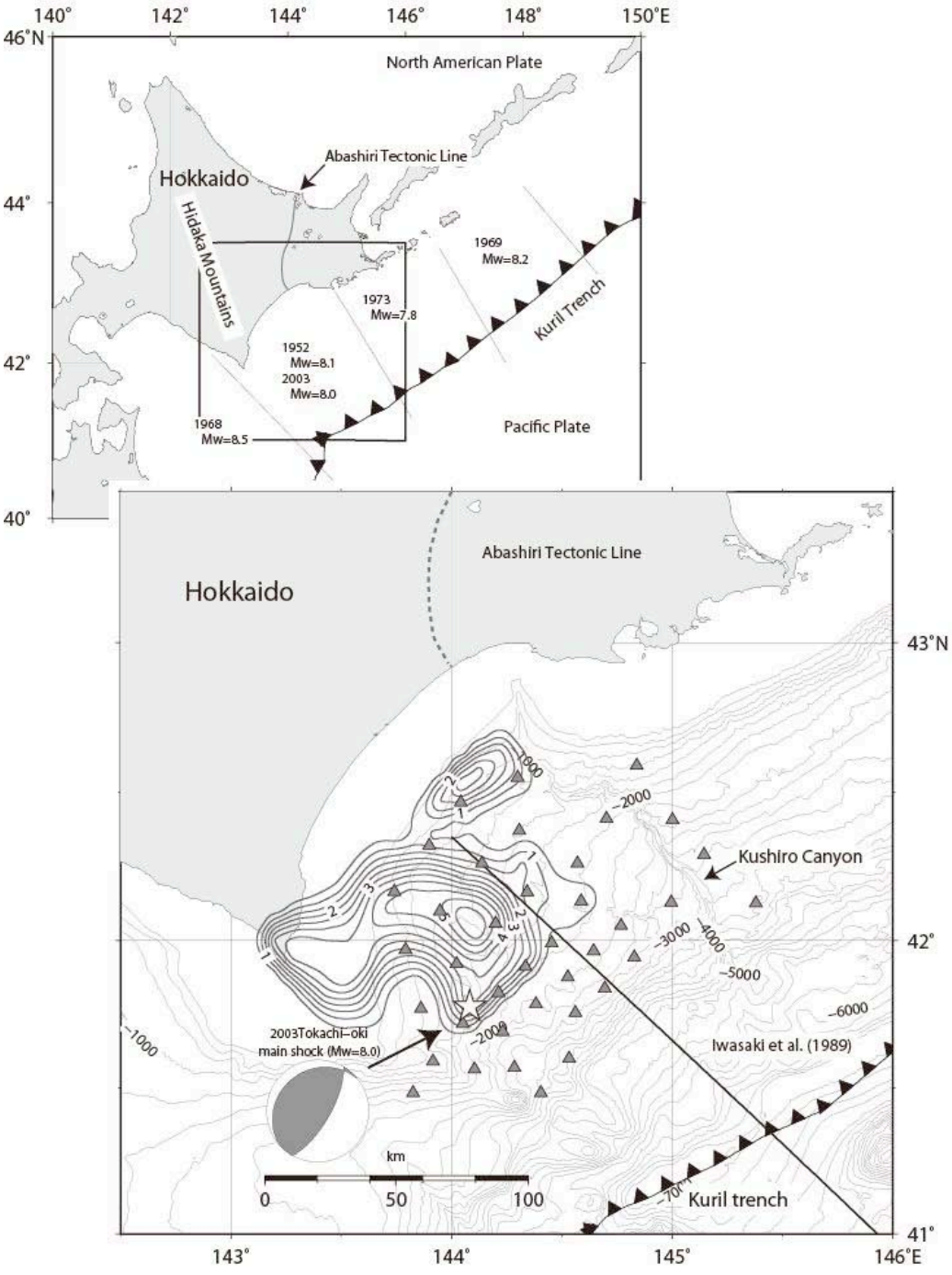
140°
142°
144°
146°
148°
150°E
46°N
44°
42°
40°
North American Plate
Abashiri Tectonic Line
Hokkaido
Hidaka Mountains
1969
Mw=8.2
1973
Mw=7.8
1952
Mw=8.1
2003
Mw=8.0
1968
Mw=8.5
Kuril Trench
Pacific Plate
Abashiri Tectonic Line
Hokkaido
43°N
42°
41°
143°
144°
145°
146°E
-1000
-2000
-3000
-4000
-5000
-6000
Kushiro Canyon
2003Tokachi-oki
main shock (Mw=8.0)
Iwasaki et al. (1989)
km
0
50
100
Kuril trench

Fig.1

692

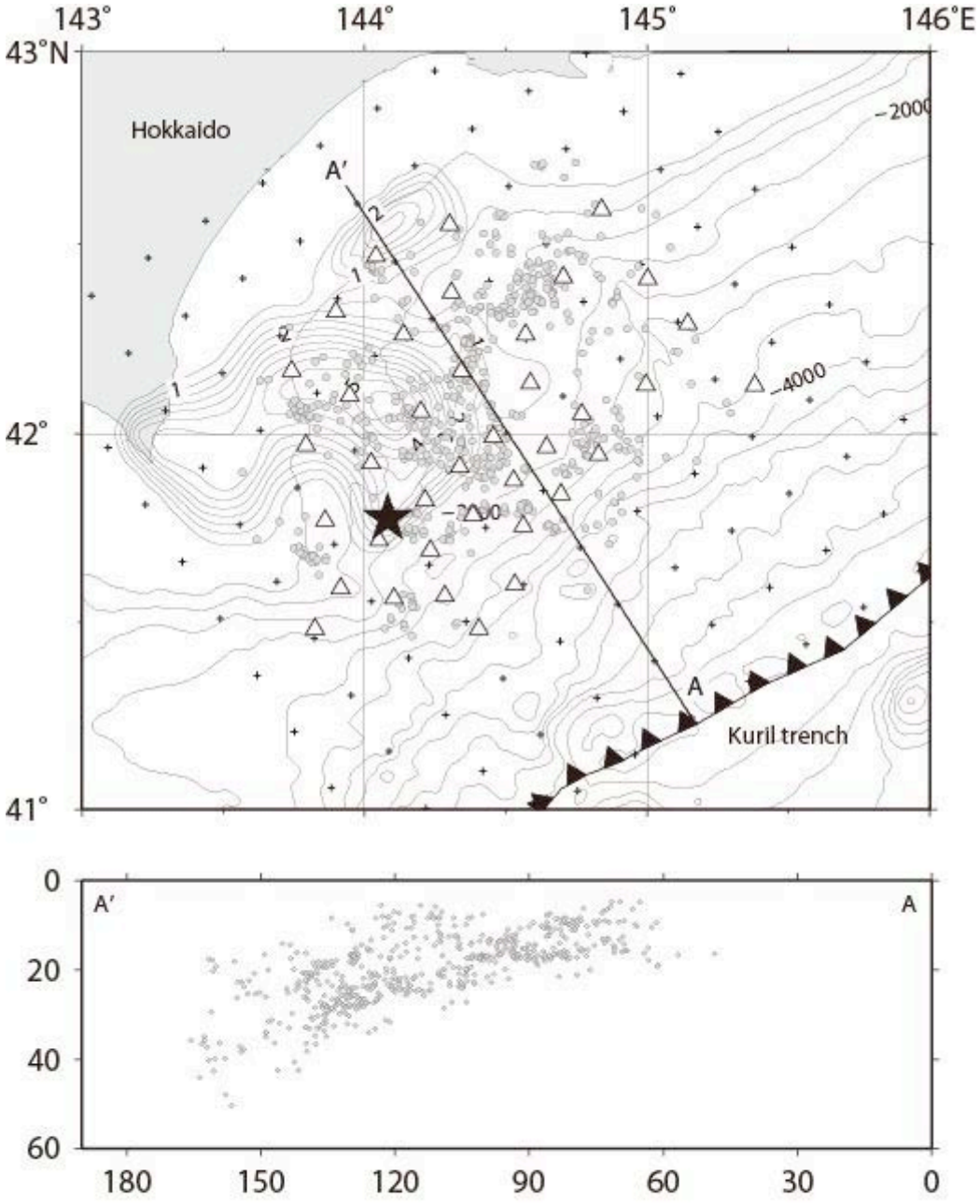
143°
144°
145°
146°E
43°N
42°
41°
Hokkaido
A′
A
Kuril trench
2000
4000
0
20
40
60
180
150
120
90
60
30
0

Fig.2

693

694

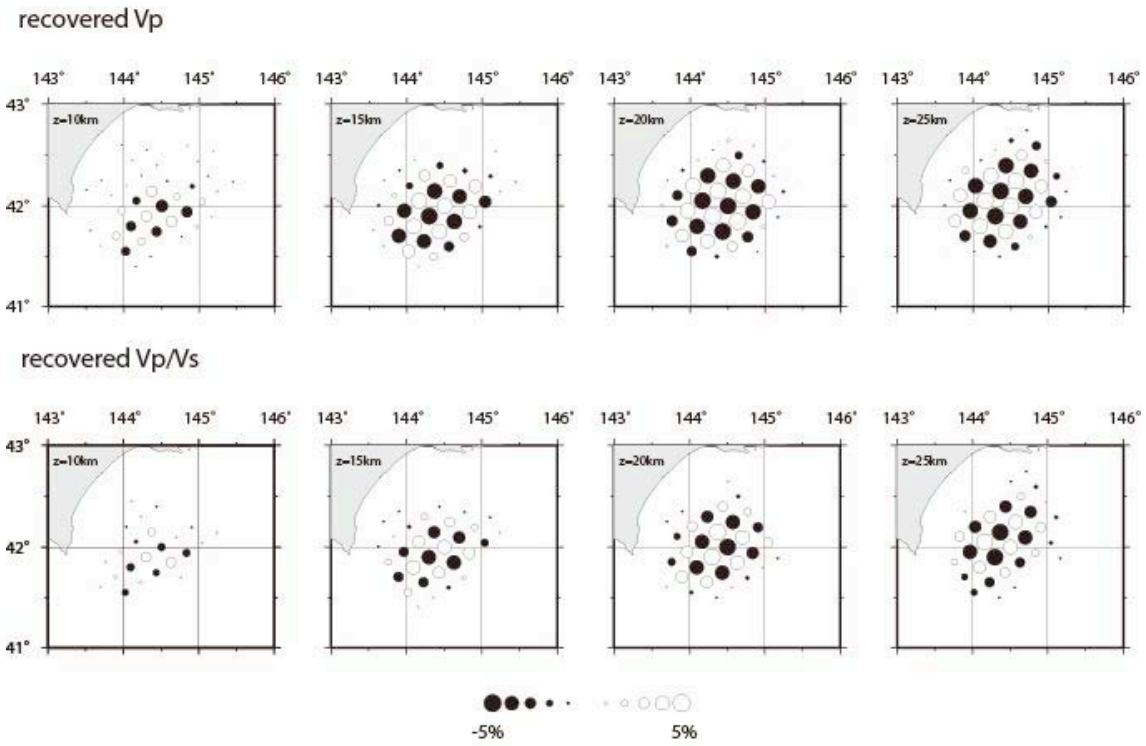
recovered Vp
143°
144°
145°
146°
43°
42°
41°
z=10km
z=15km
z=20km
z=25km
recovered Vp/Vs
-5%
5%

Fig.3

694

695

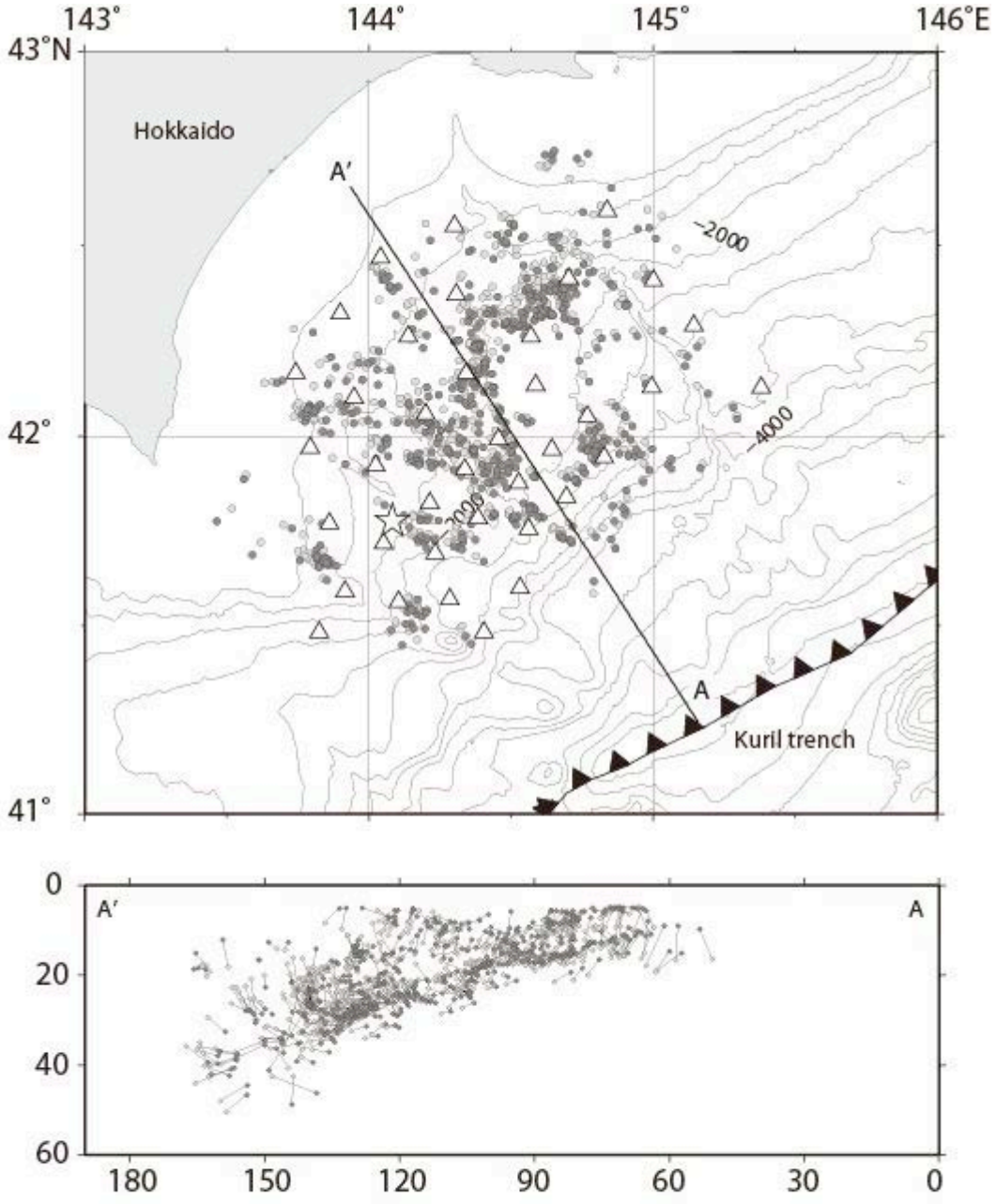
143°
144°
145°
146°E
43°N
42°
41°
Hokkaido
A′
A
−2000
−4000
−200
Kuril trench
0
20
40
60
A′
A
180
150
120
90
60
30
0

Fig.4

695

696

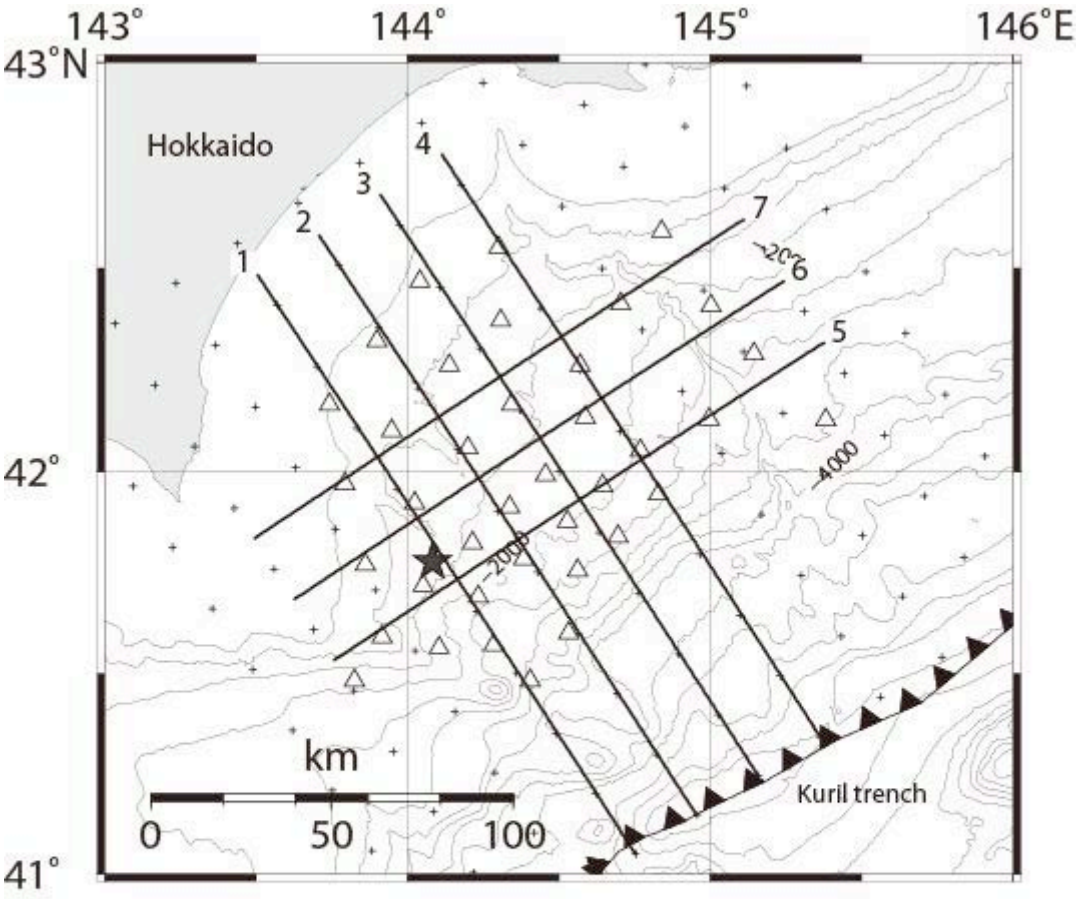
143°
144°
145°
146°E
43°N
42°
41°
Hokkaido
1
2
3
4
5
6
7
-2000
-4000
km
0
50
100
Kuril trench

Fig.5

696

697

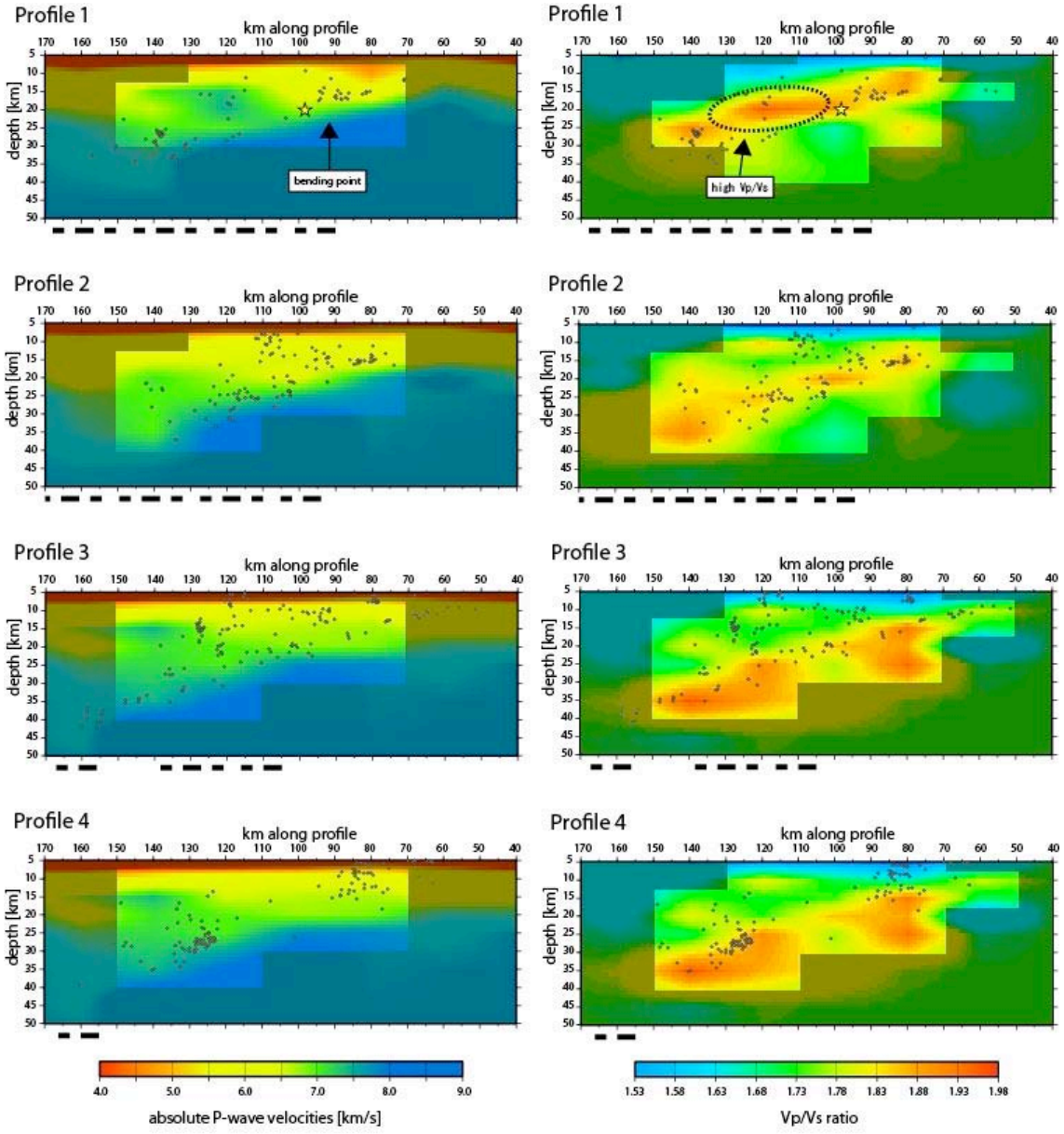
Profile 1
km along profile
depth [km]
bending point
Profile 1
km along profile
depth [km]
high Vp/Vs
Profile 2
km along profile
depth [km]
Profile 2
km along profile
depth [km]
Profile 3
km along profile
depth [km]
Profile 3
km along profile
depth [km]
Profile 4
km along profile
depth [km]
Profile 4
km along profile
depth [km]
4.0 5.0 6.0 7.0 8.0 9.0
absolute P-wave velocities [km/s]
1.53 1.58 1.63 1.68 1.73 1.78 1.83 1.88 1.93 1.98
Vp/Vs ratio

Fig.6

697

698

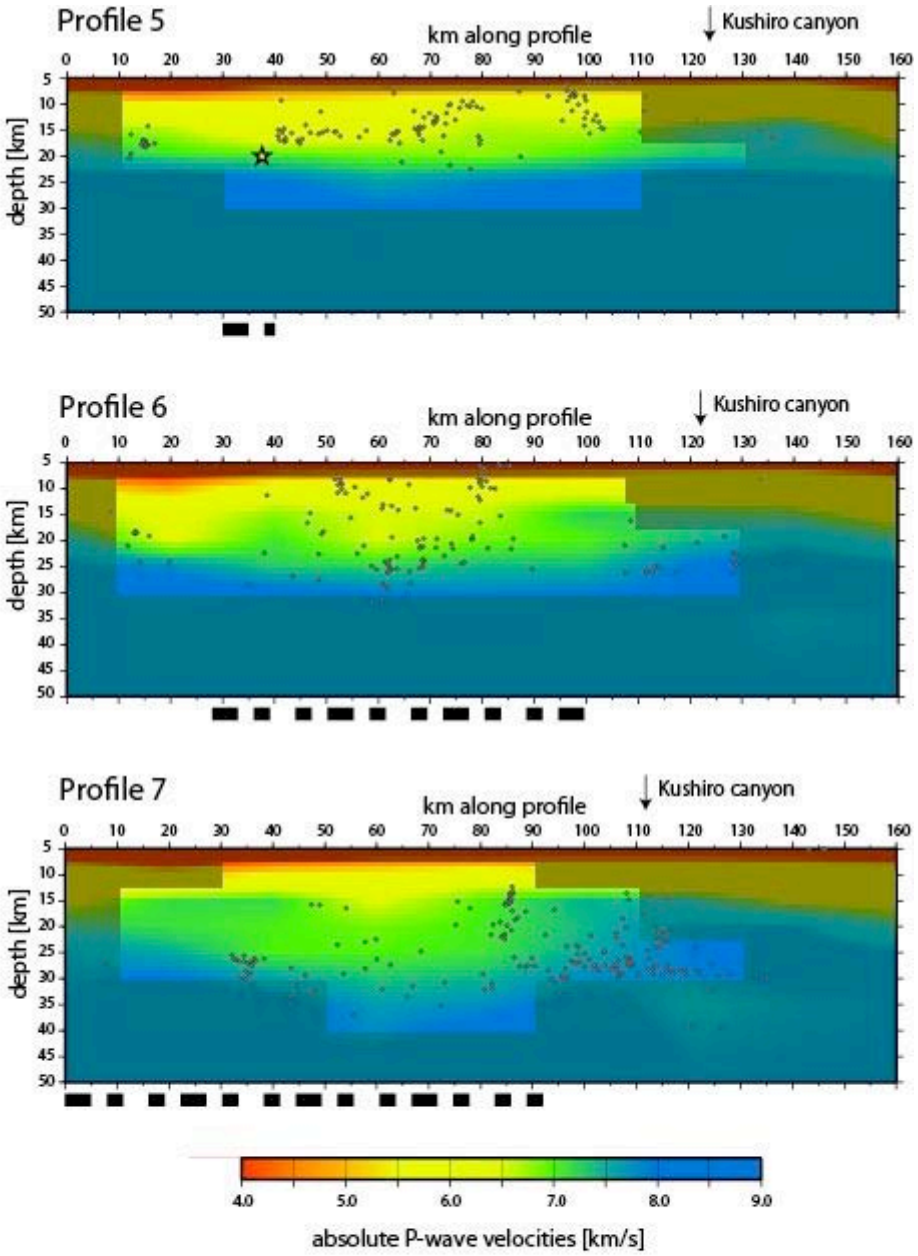
Profile 5
km along profile
Kushiro canyon
depth [km]
Profile 6
km along profile
Kushiro canyon
depth [km]
Profile 7
km along profile
Kushiro canyon
depth [km]
4.0
5.0
6.0
7.0
8.0
9.0
absolute P-wave velocities [km/s]

Fig.7

698

699

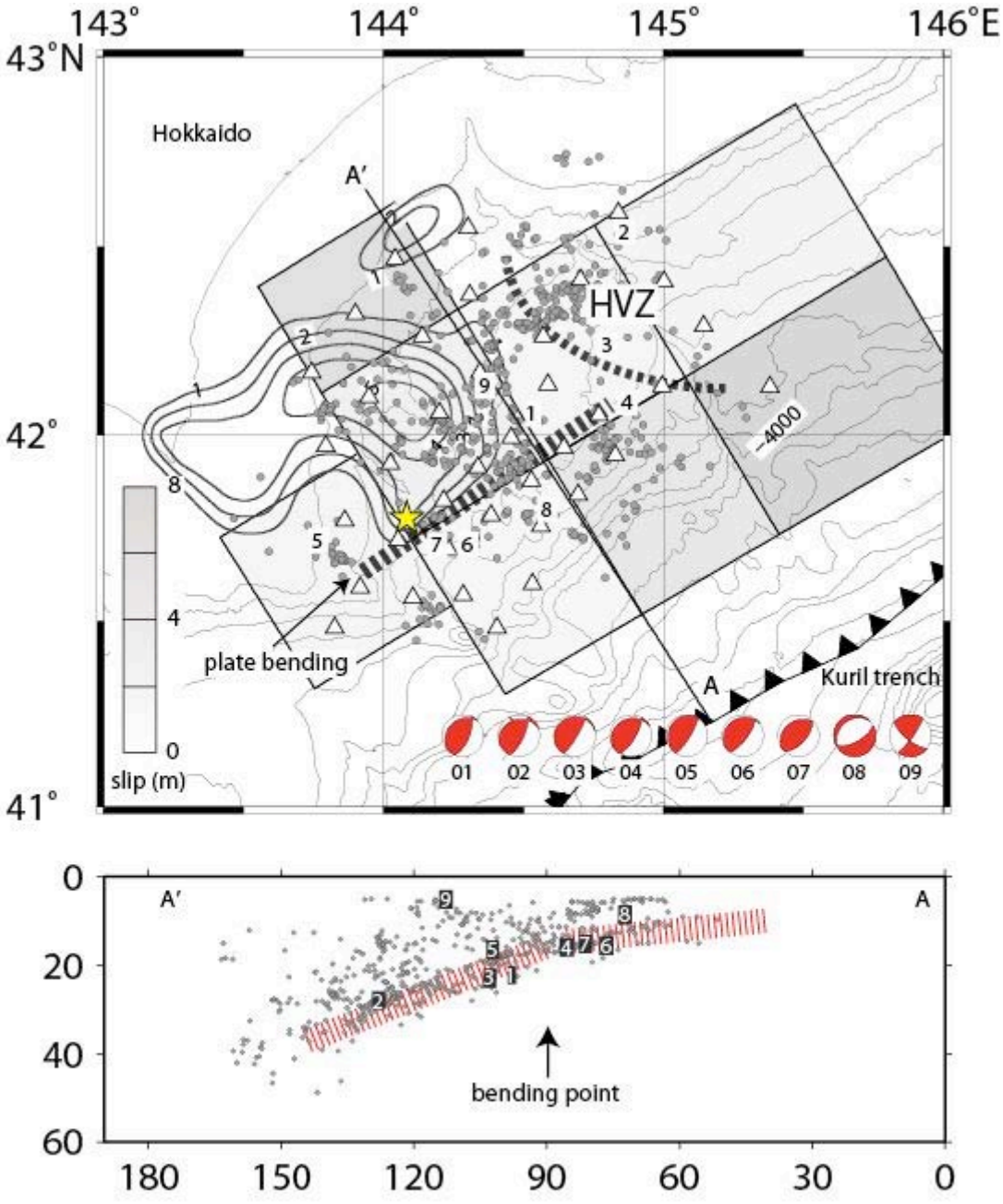
143°
144°
145°
146°E
43°N
42°
41°
Hokkaido
A′
A
HVZ
−4000
plate bending
Kuril trench
slip (m)
8
4
0
01
02
03
04
05
06
07
08
09
0
20
40
60
180
150
120
90
60
30
0
bending point

Fig.8

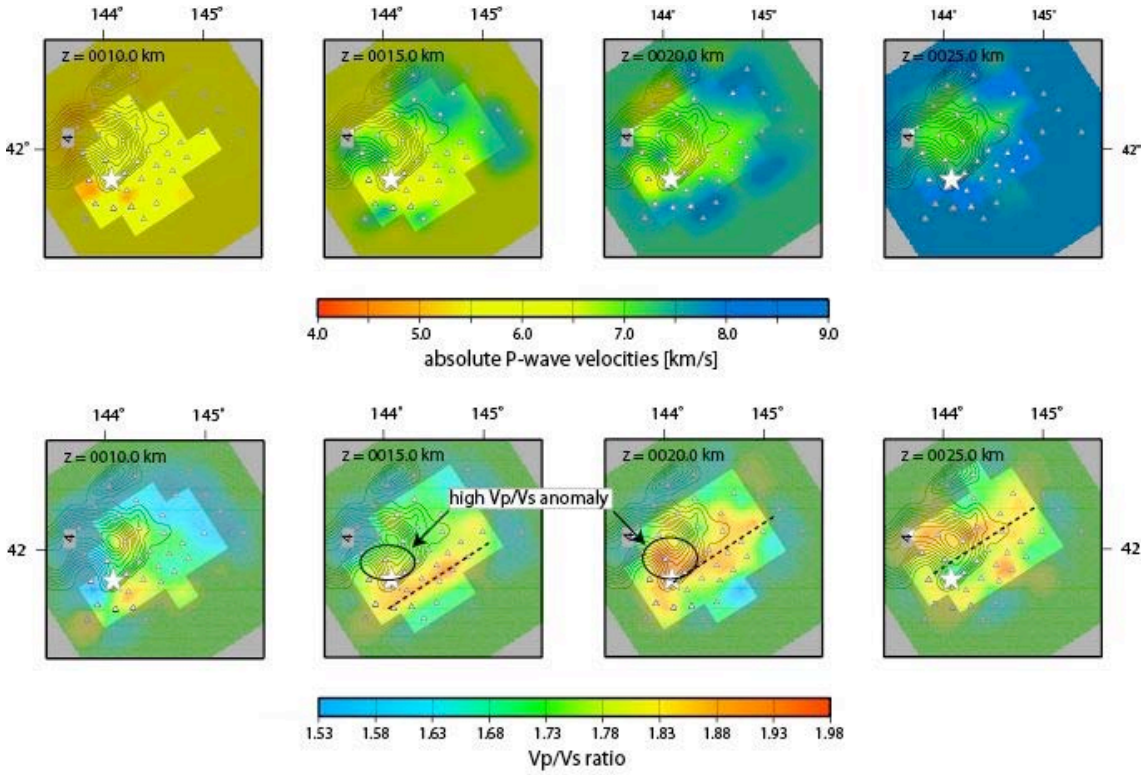
144°
145°
z = 0010.0 km
z = 0015.0 km
z = 0020.0 km
z = 0025.0 km
42°
4.0
5.0
6.0
7.0
8.0
9.0
absolute P-wave velocities [km/s]
42
high Vp/Vs anomaly
1.53
1.58
1.63
1.68
1.73
1.78
1.83
1.88
1.93
1.98
Vp/Vs ratio

Fig.9

700

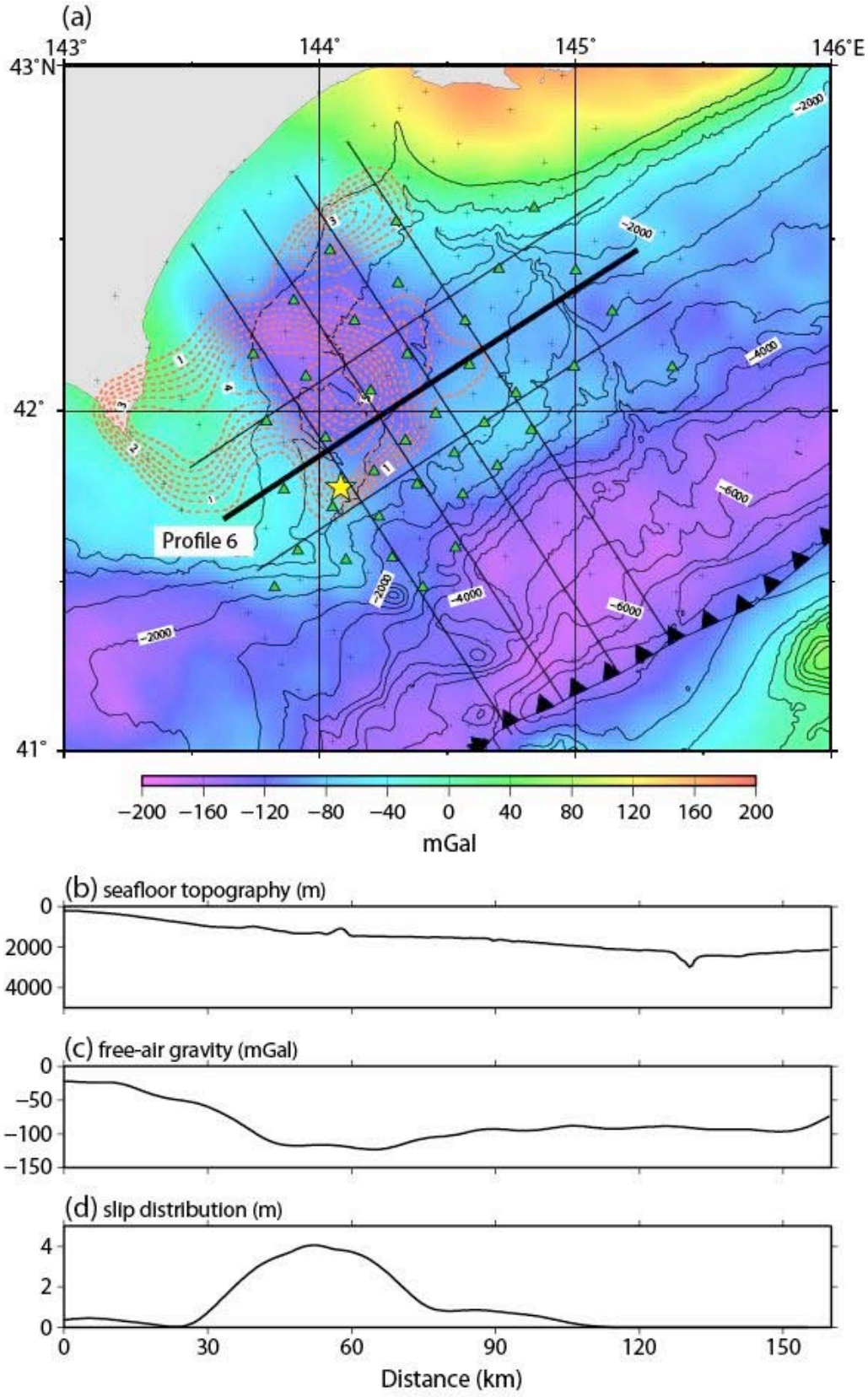
(a)
143°
144°
145°
146°E
43°N
42°
41°
Profile 6
−2000
−4000
−6000
−200 −160 −120 −80 −40 0 40 80 120 160 200
mGal
(b) seafloor topography (m)
0
2000
4000
(c) free-air gravity (mGal)
0
−50
−100
−150
(d) slip distribution (m)
4
2
0
0 30 60 90 120 150
Distance (km)

Fig.10

701

P-waves		S-waves	
RMS (s) without SC	RMS (s) with SC	RMS (s) without SC	RMS (s) with SC
0.361	0.051	1.769	0.198

Table 1

Depth (km)	Vp (km/s)	Vs (km/s)	Vp/Vs
-5.00	2.00	1.16	1.73
0.00	2.00	1.16	1.73
5.00	3.00	1.73	1.73
10.00	5.40	3.12	1.73
15.00	6.60	3.82	1.73
20.00	7.30	4.22	1.73
25.00	8.00	4.62	1.73
35.00	8.00	4.62	1.73
45.00	8.00	4.62	1.73
55.00	8.00	4.62	1.73
200.00	8.00	4.62	1.73

Table 2.